

## NON-DESTRUCTIVE EVALUATION OF THE PULL-OFF ADHESION OF CONCRETE FLOOR LAYERS USING RBF NEURAL NETWORK

Łukasz SADOWSKI

*Institute of Building Engineering, Wrocław University of Technology, Wybrzeże Wyspiańskiego 27, 50-370, Wrocław, Poland*

Received 28 Sep. 2012; accepted 22 Mar. 2013

**Abstract.** The interlayer bond is one of the primary qualities assessed during an inspection of floor concrete workmanship. The measure of this bond is the value of pull-off adhesion  $f_b$  determined in practice by the pull-off method. The drawback of this method is that the tested floor is damaged in each of the test points and then needs to be repaired. This drawback can be overcome by developing a way which will make it possible to test floors in any point without damaging them locally. In this paper it is proposed to evaluate the pull-off adhesion of the top layer to the base layer in concrete floors by means of the radial basis function (RBF) artificial neural network using the parameters evaluated by the non-destructive acoustic impulse response technique and the non-destructive optical laser triangulation method. Presented RBF neural network model is useful tool in the non-destructive evaluation of the pull-off adhesion of concrete floor layers without the need to damage the top layer fragment from the base.

**Keywords:** artificial intelligence; concrete floor; interlayer bond; acoustic methods; impulse response technique; surface roughness.

**Reference** to this paper should be made as follows: Sadowski, Ł. 2013. Non-destructive evaluation of the pull-off adhesion of concrete floor layers using RBF neural network, *Journal of Civil Engineering and Management* 19(4): 550–560. <http://dx.doi.org/10.3846/13923730.2013.790838>

### Introduction

One of the serious defects occurring in floors is the lack of adhesion at the base layer/top layer interface (Błaszczynski *et al.* 2006; Łowińska-Kluge, Błaszczynski 2012). Adhesion is the ability of different materials to stick to each other. According to Courard (2000), Fiebrich (1994), Sasse (2007), adhesion proper, connected with chemical and physicochemical interactions (hydrogen bonds and van der Waals bonds), and mechanical adhesion, connected with the mechanical anchoring of the material of one layer in the pores and surface irregularities of another layer, are distinguished. According to Czarnecki and Chmielewska (2005) and Łukowski (2005), the main factors determining the level of adhesion proper are: the compressive strength of the base concrete and the latter's temperature and moisture content. Also, the physical properties of the materials which are to be joined, such as viscosity, wettability, bond shrinkage, thermal expansion and elastic modulus are vital. However, it is the development of the contacting surfaces, the porosity of the substrate and the presence of micro-cracks in the latter which have the greatest influence on the level of mechanical adhesion. According to

Piotrowski (2009), mechanical adhesion has the decisive influence on the quality of the bond between concrete layers.

The interlayer bond is one of the primary qualities assessed during an inspection of floor concrete workmanship. The measure of this bond is the value of pull-off adhesion  $f_b$  determined in practice by the pull-off method. The method is both qualitative – defects (e.g. no adhesion) at the interface between the layers can be detected – and quantitative – the value of pull-off adhesion  $f_b$  can be determined. According to this method, adhesion is measured by measuring the ultimate load (pull-off force) using a servomotor with a pressure gauge. For this purpose cores 50 mm in diameter are drilled in the floor top layer and pulled off (via steel discs stuck onto them) from the surface of the base layer. A value of top layer/base layer adhesion of no less than 0.5 MPa determined in this way is an indicator of good floor workmanship (Courard *et al.* 2011; Czarnecki, Chmielewska 2011).

The effectiveness of the above semi-non-destructive method to a large extent depends on the number of measuring points. According to standard EN 12504-3:2006, this number should be 1 measurement

per 3 m<sup>2</sup> of floor. This requirement is rather onerous in the case of large-area floors, considering that the floor is damaged in each of the measuring points, as shown in Figure 1. Each such damage must be repaired after the test. Consequently, in practice the number of measuring points tends to be reduced. Therefore there is a need for a more effective method devoid of the above drawback, which will make it possible to test the

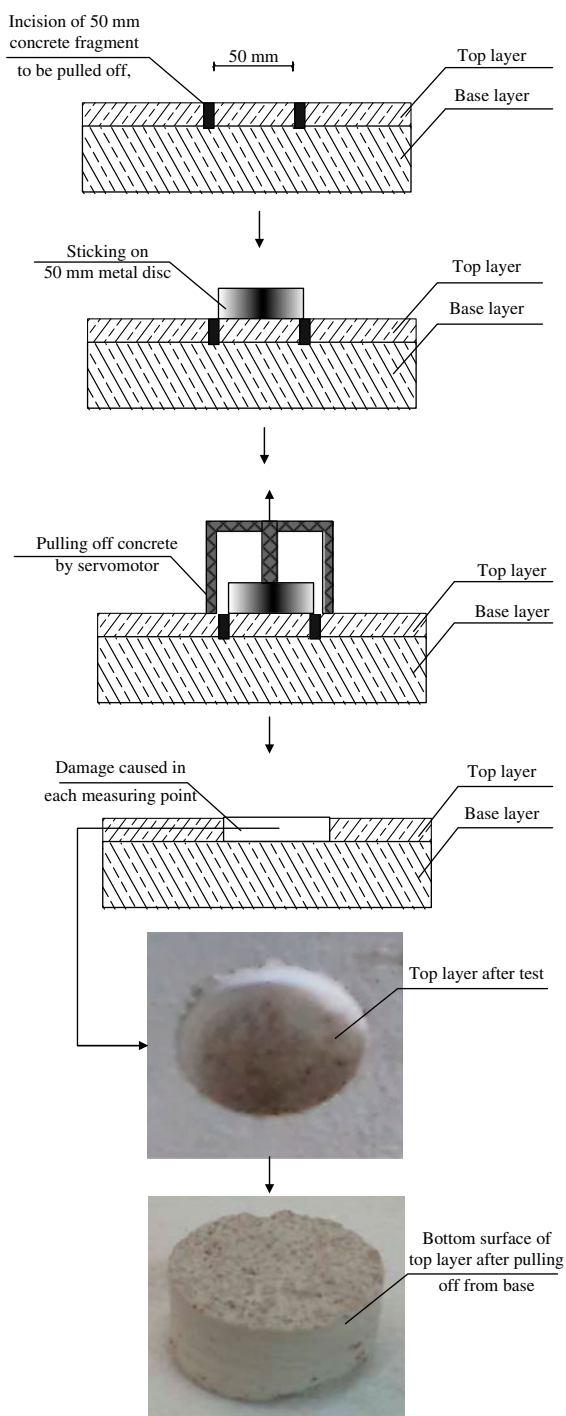


Fig. 1. Sequence showing how floor top concrete layer is damaged by pulling off  $\phi$  50 mm piece of it from base, using semi-non-destructive method

floor in any place without damaging the tested surface.

The proper preparation of the base layer, which can be described in terms of surface roughness, is a major determinant of pull-off adhesion  $f_b$  at the interface between the concrete layers in a floor (Kuzinovski *et al.* 2009; Mathia *et al.* 2011). It has been demonstrated that there is a correlation between roughness parameters and pull-off adhesion (Garbacz *et al.* 2006; Naderi, Ghodousian 2012; Siewczyńska 2012). From the point of view of the non-destructive assessment of the quality of the interlayer bond in concrete floors, the surface roughness parameters determined by the non-destructive optical laser triangulation (scanning) method prior to base surface concreting can be useful (Gonzalez-Jorge *et al.* 2012; Grzelka *et al.* 2010; Reiner, Stankiewicz 2011). Literature reports indicate that 3D parameter values determined by analysing the spatial image of the tested concrete surface (Fig. 2) can be used in order to non-destructively assess the interlayer bond in concrete floors. Such parameters as: arithmetical mean height of the surface  $S_a$ , root mean square height of the surface  $S_q$  or surface bearing index  $S_{bi}$  are increasingly often used in civil engineering to describe concrete surface roughness (Grzelka *et al.* 2011; Ourahmoune *et al.* 2011; Sadowski 2012; Werner *et al.* 2013).

Literature reports indicate that also acoustic methods can be useful for assessing the pull-off adhesion of the concrete layers in floors (Beutel *et al.* 2008; Cerniglia *et al.* 2010; Gorzelańczyk 2012; Goszczyńska *et al.* 2012; Hoła, Schabowicz 2010; Matsuyama *et al.* 2010). As opposed to the semi-non-destructive pull-off method, they supply information about the tested element without disturbing its structure. An example of their application can be found in the paper (Hoła *et al.* 2011) dealing with the assessment of the interlayer bond in concrete floors, using the zero/one (no bond/bond) system, in order to identify concrete floor areas in which delamination at the top layer/base layer interface occurred.

From among non-destructive methods, the acoustic impulse response technique is suitable for the considered purpose. The test equipment used in this method is shown in Figure 3. According to the papers (Davis 2003; Hoła, Sadowski 2012; Ottosen *et al.* 2004), the parameters most useful in this technique are: average mobility  $N_{av}$  and stiffness  $K_d$ . In Hoła and Sadowski (2012) an attempt was made to determine reliable correlations between the individual parameters recorded by the impulse response technique and the pull-off adhesion determined by the pull-off method. However, the attempt was unsuccessful because of the low values of the coefficient of determination.

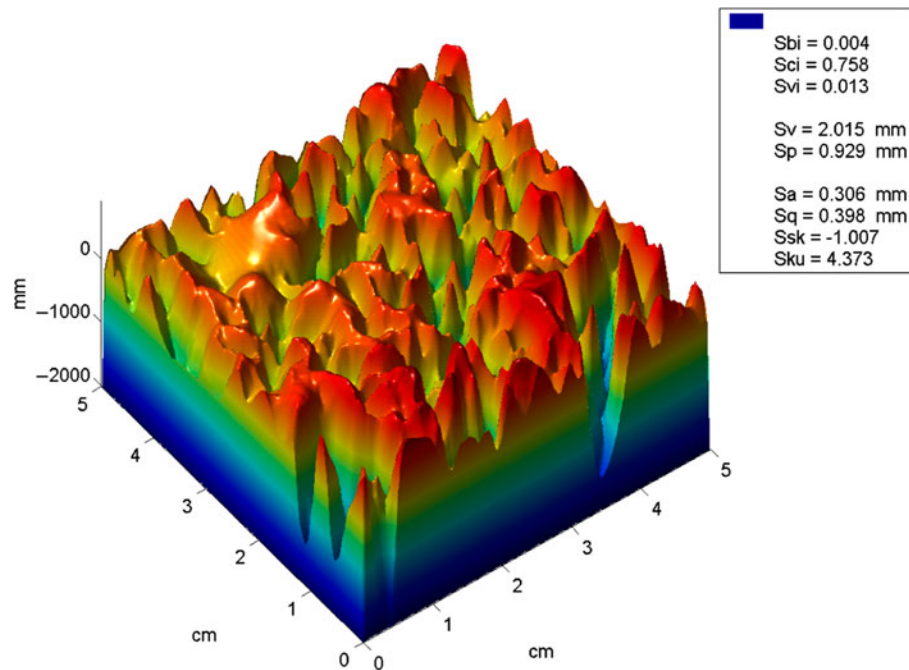


Fig. 2. Typical spatial image of scanned surface, and surface roughness parameters

Considering the above, it seems reasonable to search for a new method of identifying the pull-off adhesion of the concrete layers in floors on the basis of several parameters describing base layer roughness and parameters determined on the surface of the floor top layer by the impulse response technique. In order to correlate a larger number of parameters it was proposed to use artificial neural networks (ANNs) (Kwaśnicka 2005). ANNs have been increasingly often used in civil engineering (Altun *et al.* 2008; Bilgehan *et al.* 2012; Gencil *et al.* 2011; Hasanzadehshooiili *et al.* 2012; Hoła, Schabowicz 2005; Shaw *et al.* 2005; Kaczmarczyk, Waszczyszyn 2007; Sadowski 2013;

Zapata *et al.* 2012). One of the most often used ANNs are radial basis function (RBF) ANNs. The advantages they offer are the much simplified selection of the input layer structure and the much simpler and shorter training process requiring less computing power. RBF neural networks have already been applied in civil engineering (Kaliszuk *et al.* 2001; Kappatos, Dermatas 2007; Kim *et al.* 2006; Schabowicz 2003; Zhang *et al.* 2011). They were also used in this research to non-destructively evaluate the pull-off adhesion of the concrete layers in floors on the basis of parameters assessed by non-destructive methods: the optical laser triangulation method and the acoustic impulse response technique.

One can suppose that the parameters in the particular test points on the top layer surface recorded by non-destructive acoustic methods together with the concrete base surface roughness parameters previously non-destructively determined in the same test points, compared with the values of pull-off adhesion  $f_b$  of the top layer to the base layer determined in the same test points by the semi-nondestructive pull-off method, can make up a database for the training and testing of ANNs. Once an ANN is trained and tested it can be used to generate pull-off adhesion values for any tested area in a given floor on the basis of the parameters recorded using the non-destructive methods.

The aim of this paper is to demonstrate that pull-off adhesion of the top layer to the base layer in any point of a concrete floor can be identified by the RBF neural network on the basis of the base layer surface roughness parameters evaluated by the optical laser triangulation method and the parameters evaluated



Fig. 3. Test equipment used in non-destructive acoustic impulse response technique

on the floor surface by the acoustic impulse response technique.

### 1. Methods used

In this section the methods used in this research, i.e. the non-destructive impulse response technique, the non-destructive optical technique and the semi-destructive pull-off method, are briefly described. Also the ANN employed is described.

#### 1.1. Non-destructive impulse response technique

The non-destructive impulse response technique consists in generating an elastic wave in a tested element by means of a rubber tipped calibrated hammer. The frequency of the generated elastic wave is in a range of 1–800 Hz and the excitation extends to about 50 cm around the measuring point. Hammer strikes are executed in selected measuring points. The signal of the elastic wave propagating in the tested element is registered by a geophone and simultaneously amplified by an amplifier. The signals recorded during the tests are subsequently processed using the dedicated Impulse Response s'Mash software installed on a laptop. The measuring set used in the impulse response technique is shown in Figure 4.

The registered parameters are: average mobility  $N_{av}$ , stiffness  $K_d$ , mobility slope  $M_p/N$ , average mobility times mobility slope  $N_{av} \cdot M_p$  and voids index  $v$ . Two of the above parameters, which are most often used to locate floor areas lacking adhesion (Hoła, Sadowski 2012), are used in this paper. According to Hoła *et al.* (2011), Ottosen *et al.* (2004), they are:  $N_{av}$  – the average mobility of vibrations  $N$ , defined as a ratio of maximum velocity  $w_{max}$  to maximum elastic wave  $F_{max}$  generated by the hammer:

$$N_{av} = \frac{w_{max}}{F_{max}}. \quad (1)$$

$K_d$  – the cotangent of mobility curve inclination angle  $\alpha$  in a frequency range of 0–80 Hz:

$$K_d = ctg\alpha. \quad (2)$$

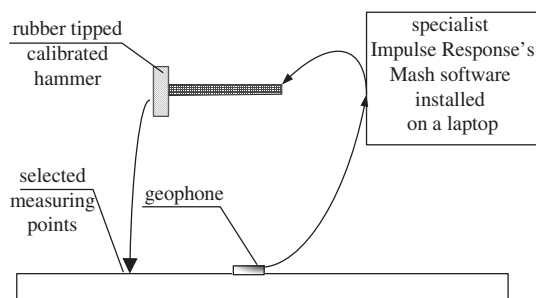


Fig. 4. Schematic of the non-destructive impulse response technique

#### 1.2. Non-destructive optical technique

The set for surface roughness examinations by means of the optical technique comprises: a laser distance sensor mounted on a linear drive with a guide, a controller incorporating an amplifier, and a laptop. The IVC Studio 3.1 S.R.2 software installed on the laptop was used in the optical investigations, carried out (in previously determined measuring points) using a 161×55×60 mm IVC-2D camera with a resolution of 1028×768 pixels, mounted on a guide (Fig. 5).

Scanning is effected by manually shifting the head above the measuring area during which several surface profiles, separated from one another by a distance of 0.1 mm, are being recorded with a resolution of 0.074 mm. As a result, a 3D image of the concrete surface is obtained. The data from the camera after prefiltration are sent to the laptop to be archived. The dedicated software installed on the laptop is used to process the data and to generate the values of such surface roughness parameters as:  $S_a$  – the average arithmetic deviation of the surface from reference surface  $A$ , expressed by the equation:

$$S_a = \frac{1}{A} \sum_{j=1}^N \sum_{i=1}^M z(i,j), \quad (3)$$

$S_q$  – the rms deviation of the surface from reference surface  $A$ :

$$S_q = \sqrt{\frac{1}{A} \sum_{j=1}^N \sum_{i=1}^M z^2(i,j)}, \quad (4)$$

$S_{bi}$  – a surface bearing index, which is a ratio of rms surface roughness deviation  $S_q$  to  $\eta_{0.05}$ , where  $\eta_{0.05}$  is the level separating the peak surface roughness from the core for a default value of 5%:

$$S_{bi} = \frac{S_q}{\eta_{0.05}}. \quad (5)$$

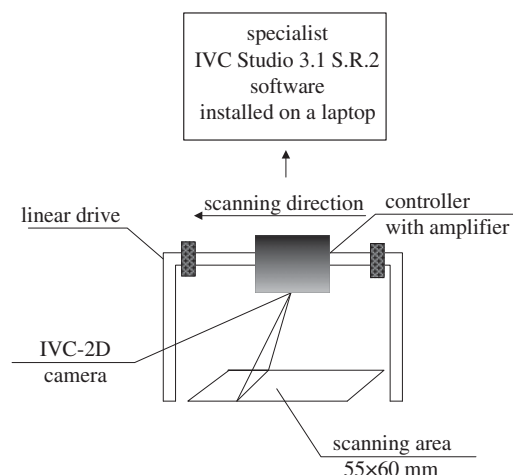


Fig. 5. Schematic of the non-destructive optical technique

The above three parameters determinable using the non-destructive optical technique were used in this research as the input parameters for training, testing and verifying the ANN.

As part of this research an attempt was made to non-destructively determine pull-off adhesion  $f_b$  in any measuring point, leaving the surface of the tested concrete floor intact.

### 1.3. Semi-destructive pull-off method

The pull-off method, illustrated in Figure 6, is used to determine the adhesion of concrete floor layers. The method belongs to a group of semi-nondestructive methods. In this method, the adhesion of the top layer to the base layer is evaluated by measuring the pull-off force with a servomotor equipped with a pressure gauge. For this purpose cores 50 mm diameter are drilled in the topping and pulled off from the base layer.

The method is both qualitative, since it can indicate a defect (e.g. lack of adhesion) at the interface between the layers, and quantitative since using it one can determine pull-off adhesion  $f_b$ .

In this method,  $f_b$  is calculated from the equation:

$$f_b = \frac{4 \cdot F_b}{\pi \cdot D_f^2}, \quad (6)$$

where:  $F_b$  – failure load, N;  $D_f$  – an average sample diameter, m.

### 1.4. RBF neural network

The main purpose of RBF neural networks is to approximate functions of several variables in order to map a set of input variables into a set of output variables (Moody, Darken 1989; Rafajłowicz, Skubalska-Rafajłowicz 2009; Xie *et al.* 2012; Yao *et al.* 2012). The approximation in this case is global since it is simultaneously performed for many neurons. In RBF neural networks a hidden neuron executes a function radially changing around a selected centre, assuming nonzero values only in the neighbourhood of this centre, as shown in Figure 7.

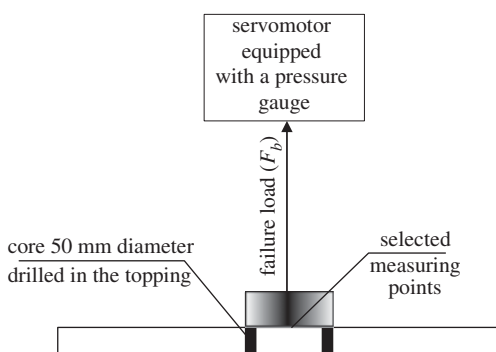


Fig. 6. Schematic of the semi-destructive pull-off method

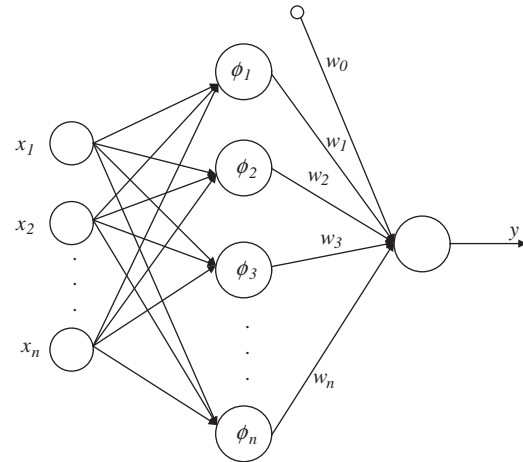


Fig. 7. Schematic of RBF neural network

The effectiveness of a neural network is usually evaluated using such correlation error measures as:

– linear correlation coefficient  $R$ :

$$R_i = \frac{\left( P \sum_{p=1}^P d_i^p y_i^p - \sum_{p=1}^P d_i^p \sum_{p=1}^P y_i^p \right)^2}{\left( P \sum_{p=1}^P (d_i^p)^2 - \left( \sum_{p=1}^P d_i^p \right)^2 \right) \cdot \left( P \sum_{p=1}^P (y_i^p)^2 - \left( \sum_{p=1}^P y_i^p \right)^2 \right)}, \quad (7)$$

– relative error (RE):

$$RE = \frac{|y_i^p - \bar{y}_i^p|}{y_i^p}, \quad (8)$$

where:  $P$  – the number of training patterns;  $M$  – the number of inputs;  $d_i^p$  – the  $i$ -th expected value for pattern  $p$ ;  $y_i^p$  – the  $i$ -th value of the response from the network to pattern  $p$ ;  $\bar{y}_i^p$  – the average value of the network response to pattern  $p$ .

## 2. Experimental details

Two  $2500 \times 2500$  mm model concrete floor specimens consisting of a 25 mm thick top layer laid on a 125 mm thick base were tested. The top layer was made of grade C20/25 cement mortar. The base layer was made of grade C30/37 concrete with a maximum aggregate grading of 8 mm. Up to the time of the tests the specimens had been stored in a laboratory at a temperature of  $20 \pm 5$  °C. The base layer was laid on a 100 mm thick layer of sand. The specimens were tested using the non-destructive impulse response technique and the semi-destructive pull-off method after the top layer had cured for 90 days.

Four ways of preparing the base layer surface, denoted with Roman numerals I–IV (Fig. 8) were proposed. The surface of the top layer of each model specimen was marked, a  $1500 \times 1500$  mm test area was outlined on the surface and a grid of measuring points

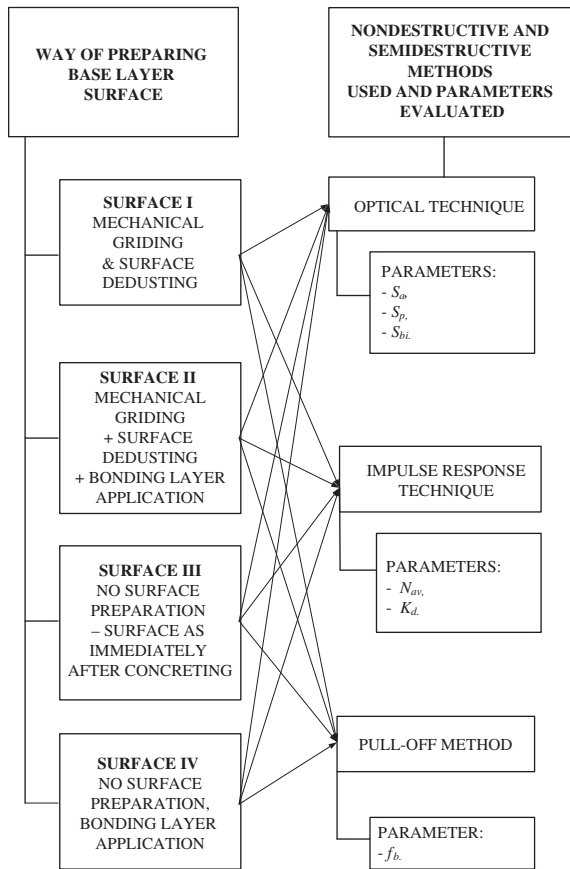


Fig. 8. Combinations of ways of preparing base layer surface and non-destructive and semi-destructive methods with evaluated parameters

spaced at every 100 mm was marked on it (keeping a minimum distance of 500 mm from the edge). The columns were denoted with letters from A to H and the rows with numbers from 1 to 16. In total 128 measuring points were marked on each of the surfaces.

The non-destructive impulse response test consisted in generating (with the calibrated hammer) an elastic wave in each point of the measuring grid



Fig. 9. Testing by means of non-destructive impulse response technique

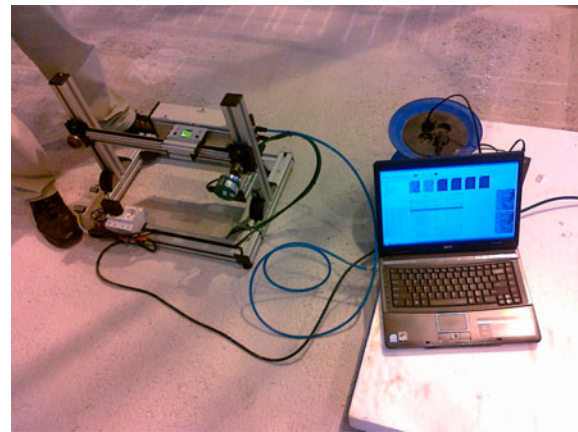


Fig. 10. Testing by means of non-destructive optical technique

marked on the floor's surface (Fig. 9). As a result of the test, the values of characteristic acoustic parameters  $N_{av}$  and  $K_d$  (their names are given in Fig. 5) in each of the points were obtained.

The non-destructive optical tests consisted in scanning the profiles of a  $55 \times 60$  mm base layer from a distance incrementally increasing by 0.1 mm (Fig. 10). As a result, a 3D image of the concrete surface within the scanned area was obtained. The data were processed using the dedicated IVC Studio 3.1 S.R.2 software installed on the laptop and the values of the concrete surface roughness parameters were displayed.

The semi-non-destructive pull-off tests consisted in determining the adhesion of the top layer to the base layer by measuring the pull-off force by means of a servomotor with a digital pressure gauge. For this purpose  $\phi$  50 mm cores were drilled in the top layer in the same points in which previously the optical tests and the impulse response tests had been carried out and the cores were pulled off from the surface of the base layer (Fig. 11).

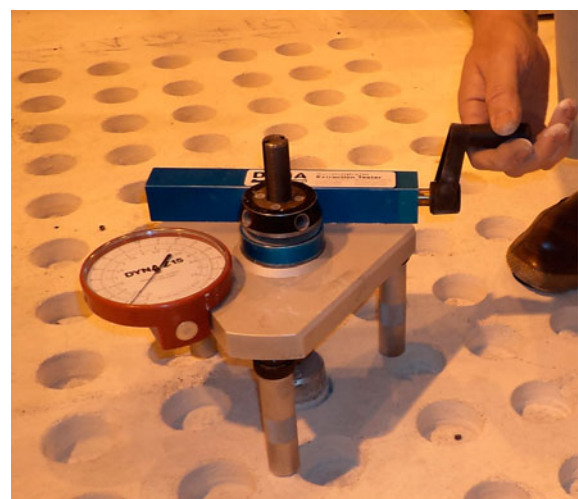


Fig. 11. Testing by means of semi-nondestructive pull-off method

### 3. Database

The 472 test results were subjected to statistical analysis, whereby the database was reduced to 460 results. The input variables obtained in this way were randomly divided into training data, testing data and verification data. From the 460 input variables, 322 results were selected for training, 69 for testing and 69 for verification. Orthogonal-least-square learning has been used for this purpose. Exemplary test results, determined by the non-destructive impulse response technique, the non-destructive optical technique and the semi-destructive pull-off method, used for the training, testing and verification of the ANN are listed in Table 1.

An RBF neural network model with one hidden layer having architecture 5-30-1 was found to be optimal for the non-destructive evaluation of pull-off adhesion (Fig. 12).

### 4. Test results and their analysis

In section 4.1 the results of training and testing the RBF neural network with 30 hidden layer neurons are presented. In section 4.2, the experimental verification of the RBF neural network is described.

#### 4.1. Results of neural network training and testing

Figures 13 and 14 show the dependencies between experimentally determined pull-off adhesion  $f_b$  and pull-off adhesion  $f_{c,b}$  identified by the RBF neural network with 30 hidden layer neurons during its training and testing. Thirty hidden layer neurons were selected because for this number RE for training and testing was the lowest and linear correlation coefficient  $R$  was the highest. Figures 15 and 16 show bar charts of RE for training and testing.

The dependence between experimentally determined pull-off adhesion  $f_b$  and pull-off adhesion  $f_{c,b}$

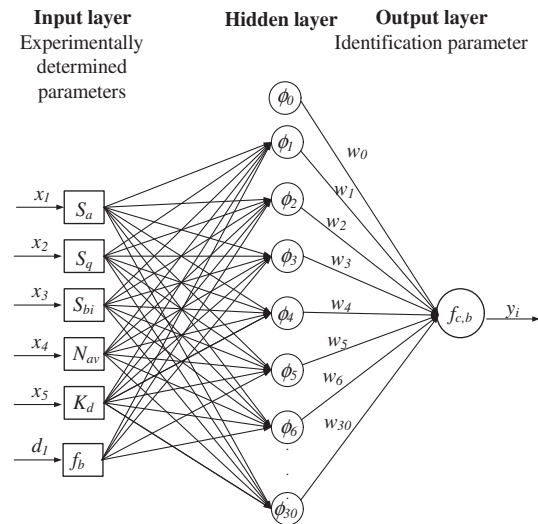


Fig. 12. Schematic of structure of RBF neural network employed for non-destructive evaluation of pull-off adhesion

identified by the neural network during its training is shown in Figure 13. The dependence between experimentally determined pull-off adhesion  $f_b$  and pull-off adhesion  $f_{c,b}$  identified by the neural network during its testing is shown in Figure 14.

The above results show that regardless of the base layer preparation, the RBF neural network correctly maps the training data and correctly identifies the testing data, as evidenced by the location of the points along the regression line corresponding to the ideal mapping. Moreover, high linear correlation coefficients  $R$  were obtained for both training and testing: 0.8175 and 0.8225, respectively, indicating that the fit has a high degree of precision.

Bar charts of RE for pull-off adhesion  $f_b$  and  $f_{c,b}$  for training and testing are shown in respectively Figures 15 and 16. The intervals of RE are marked on the X-axis while the number of results ( $n$ ) belonging to

Table 1. Exemplary test results selected for training, testing and verification

No.	Measuring techniques with obtained parameters					
	Non-destructive impulse response technique		Non-destructive optical method			Semi-destructive pull-off method
	$N_{av}$ [m/s·N]	$K_d$ [-]	$S_a$ [mm]	$S_q$ [mm]	$S_{bi}$ [-]	$f_b$ [MPa]
1	83.574	0.018	0.427	0.577	0.002	0.890
2	106.340	0.008	0.045	0.225	0.002	0.760
3	109.968	0.032	0.052	0.472	0.001	0.740
4	108.833	0.034	0.480	0.438	0.003	0.820
5	72.270	0.036	0.307	0.403	0.003	0.940
6	63.949	0.036	0.317	0.424	0.003	0.990
7	49.703	0.068	0.077	0.241	0.004	1.070
8	51.294	0.069	0.057	0.223	0.003	1.020
9	43.399	0.039	0.359	0.478	0.002	1.070
10	70.227	0.069	0.442	0.582	0.002	1.100
460	61.741	0.048	0.592	0.793	0.002	0.920

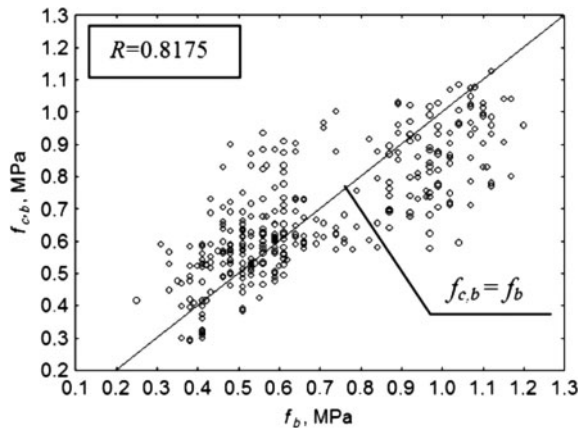


Fig. 13. Dependence between experimentally determined pull-off adhesion  $f_b$  and pull-off adhesion  $f_{c,b}$  identified by neural network during its training

the particular intervals of RE is marked on the Y-axis. According to the figures, most of the RE values are below 0.15 for both training and testing.

Presented results reflect that the RBF neural network output fit very well with the experimental values and as well illustrates that this model possess good interpolation ability.

#### 4.2. Experimental verification of neural network

In this section, the experimental verification of the neural network is described. Sixty nine test points were randomly selected. The trained neural network was fed the values of parameters  $S_a$ ,  $S_q$ ,  $S_{bi}$ ,  $N_{av}$  and  $K_d$  in each of the 69 measuring points. The trained neural network generated the value of pull-off adhesion  $f_{c,b}$  in each of the 69 points. The generated values were compared with the experimental values. Figure 17 shows the dependence between experimentally determined pull-off adhesion  $f_b$  and pull-off adhesion  $f_{c,b}$  identified by the neural network during its verification. The results show that regardless of the

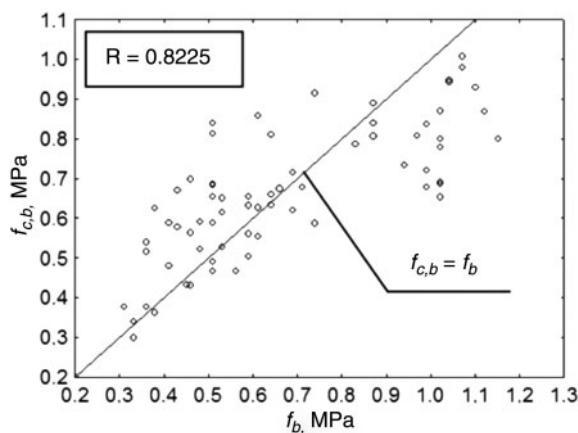


Fig. 14. Dependence between experimentally determined pull-off adhesion  $f_b$  and pull-off adhesion  $f_{c,b}$  identified by neural network during its testing

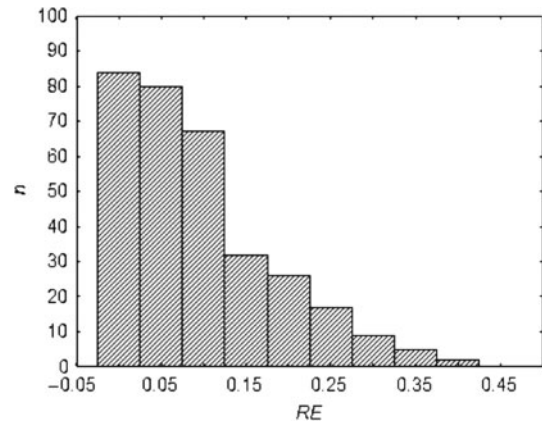


Fig. 15. Bar chart of relative error of pull-off adhesion  $f_b$  and  $f_{c,b}$  for neural network training

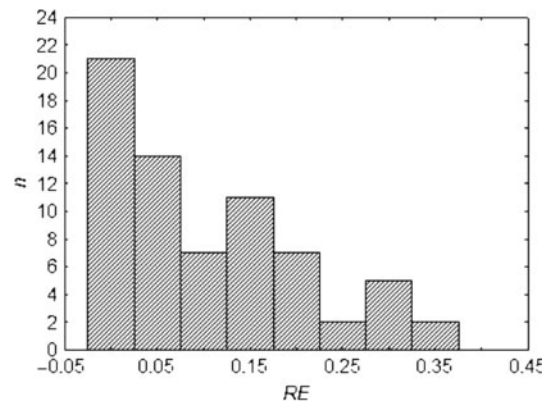


Fig. 16. Bar chart of relative error of pull-off adhesion  $f_b$  and  $f_{c,b}$  for neural network testing

way of preparing the base layer, the neural network correctly maps the randomly selected verification data, as evidenced by the location of the points along the regression line corresponding to the ideal mapping. Linear correlation coefficient  $R$  for the experimental

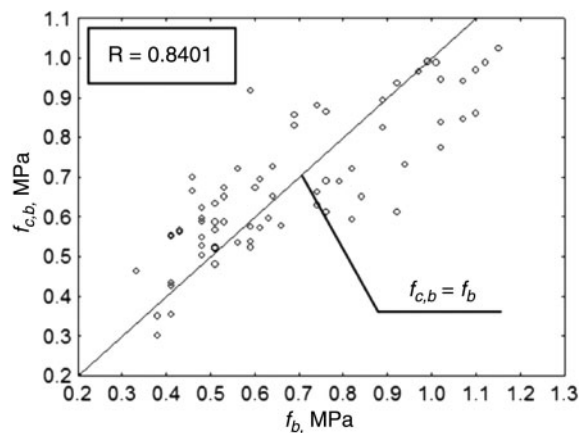


Fig. 17. Dependence between experimentally determined pull-off adhesion  $f_b$  and pull-off adhesion  $f_{c,b}$  identified by neural network during its verification



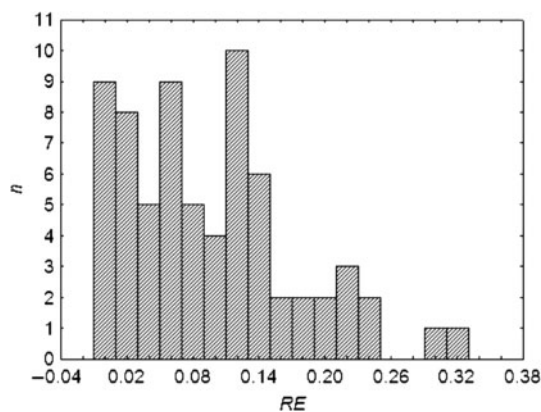


Fig. 18. Bar chart of relative RE of pull-off adhesion  $f_b$  and  $f_{c,b}$  for neural network experimental verification

verification of the neural network was found to amount to 0.8401.

Figure 18 shows a bar chart of RE of pull-off adhesion  $f_b$  and  $f_{c,b}$  for the verification of neural network. The intervals of RE are marked on the X-axis while the numbers ( $n$ ) of the results belonging to the particular intervals of RE are marked on the Y-axis. The figures show that most of the RE errors for the verification process are below 0.14.

Conversely, in the RBF neural network verification process, the predicted values of pull-off adhesion  $f_{c,b}$  plotted against the experimentally measured values of pull-off adhesion  $f_b$  indicate that the fit has a very high degree of accuracy.

## Conclusions

The experimental and numerical test results presented in this paper show that the RBF neural network with a properly matched structure and training algorithm is suitable for the non-destructive identification of pull-off adhesion  $f_{c,b}$  of the top layer to the base layer in concrete floors on the basis of parameters non-destructively evaluated using the optical laser triangulation method and the acoustic impulse response technique.

The values of this adhesion can be reliably identified by the RBF neural network on the basis of the total of five parameters determined by the non-destructive methods. The parameters are: arithmetical mean height of the surface  $S_a$ , root mean square height of the surface  $S_q$  or surface bearing index  $S_{bi}$  determined on the base layer surface by the optical laser triangulation method, and average mobility  $N_{av}$  and stiffness  $K_d$ , determined on the top layer surface by the acoustic impulse response method. The reliability of the identification is indicated by the high values of correlation coefficient  $R$ , amounting to 0.8175, 0.8225 and 0.8401 for respectively training, testing and experimental verification, and by the very

low values of RE, mostly below 0.15 for training and testing and below 0.14 for verification.

The model based on RBF neural network is useful tool in the non-destructive evaluation of the pull-off adhesion of concrete floor layers without the need to damage the top layer fragment 50 mm in diameter from the base, which is the main drawback of the pull-off method. However, it should be noted, that the proposed method is not intended to completely replace the semi-non-destructive pull-off method used today to determine the pull-off adhesion of the concrete layers in floors, but it represents a new approach to the neural identification of the values of this adhesion on the basis of five parameters: three describing base layer surface roughness, evaluated by the non-destructive optical laser triangulation method, and two evaluated on the surface of the floor top layer surface by the non-destructive acoustic impulse response technique.

## References

- Altun, F.; Kişi, Ö.; Aydin, K. 2008. Predicting the compressive strength of steel fibre addend lightweight concrete using neural network, *Computational Materials Science* 42(2): 259–265.  
<http://dx.doi.org/10.1016/j.commatsci.2007.07.011>
- Beutel, R.; Reinhardt, H.-W.; Grosse, C. U.; Glaubitt, A.; Krause, M.; Maierhofer, C.; Algernon, D.; Wigganhauser, H.; Schickert, M. 2008. Comparative performance tests and validation of NDT methods for concrete testing, *Journal of Non-destructive Evaluation* 27(1–3): 59–65.  
<http://dx.doi.org/10.1007/s10921-008-0037-1>
- Bilgehan, M.; Gürel, M. A.; Pekgökçöz, R. K.; Kısa, M. 2012. Buckling load estimation of cracked columns using artificial neural network modeling technique, *Journal of Civil Engineering and Management* 18(4): 568–579.  
<http://dx.doi.org/10.3846/13923730.2012.702988>
- Błaszczynski, T.; Jasiczak, J.; Ksist, B.; Siewczyńska, M. 2006. Aspects of bond layer role in concrete repairs, *Archives of Civil and Mechanical Engineering* 6(4): 75–87.
- Cerniglia, D.; Pantano, A.; Montinaro, N. 2010. 3D simulations and experiments of guided wave propagation in adhesively bonded multi-layered structures, *NDT & E International* 43(6): 527–535.  
<http://dx.doi.org/10.1016/j.ndteint.2010.05.009>
- Courard, L. 2000. Parametric study for the creation of the interface between concrete and repairs products, *Materials and Structures* 33: 65–72.  
<http://dx.doi.org/10.1007/BF02481698>
- Courard, L.; Lenaers, J.-F.; Michel, F.; Garbacz, A. 2011. Saturation level of the superficial zone of concrete and adhesion of repair systems, *Construction and Building Materials* 25(5): 2488–2494.  
<http://dx.doi.org/10.1016/j.conbuildmat.2010.11.076>
- Czarnecki, L.; Chmielewska, B. 2005. Uwarunkowania adhezji w złączach budowlanych [Factors affecting adhesion in building joints], *Cement Wapno Beton* 2: 74–85.

- Czarnecki, L.; Chmielewska, B. 2011. Materials and requirements for floor toppings (in Polish), in *The 23rd All-Poland Conference on Building Structure Designer's Methodology*, Poland, 11 p.
- Davis, A. G. 2003. The nondestructive impulse response test in North America: 1985–2001, *NDT & E International* 36(4): 185–193.  
[http://dx.doi.org/10.1016/S0963-8695\(02\)00065-8](http://dx.doi.org/10.1016/S0963-8695(02)00065-8)
- EN 12504-3:2006 *Testing concrete in structures – Part 3: determination of pull-off force*. 12 p.
- Fiebrich, M. 1994. Scientific aspects of adhesion phenomena in the interface mineral substrate-polymers, in *Proc. of the 2nd Bolomey Workshop, Adherence of young and old concrete*, Aedificatio, Verlag, 25–58.
- Garbacz, A.; Courard, L.; Kostana, K. 2006. Characterization of concrete surface roughness and its relation to adhesion in repair systems, *Materials Characterization* 56(4–5): 281–289.  
<http://dx.doi.org/10.1016/j.matchar.2005.10.014>
- Gencel, O.; Kocabas, F.; Gok, M. S.; Koksall, F. 2011. Comparison of artificial neural networks and general linear model approaches for the analysis of abrasive wear of concrete, *Construction and Building Materials* 25(8): 3486–3494.
- Gonzalez-Jorge, H.; Solla, M.; Armesto, J.; Arias, P. 2012. Novel method to determine laser scanner accuracy for applications in civil engineering, *Optica Applicata* 42(1): 43–53.
- Gorzelańczyk, T. 2012. Acoustically assessed influence of air pore structure on failure of self-compacting concretes under compression, *Journal of Civil Engineering and Management* 18(1): 60–70.  
<http://dx.doi.org/10.3846/13923730.2011.652982>
- Goszczyńska, B.; Świt, G.; Trąpczyński, W.; Krampikowska, A.; Tworzewska, J.; Tworzewski, P. 2012. Experimental validation of concrete crack identification and location with acoustic emission method, *Archives of Civil and Mechanical Engineering* 12(1): 23–28.  
<http://dx.doi.org/10.1016/j.acme.2012.03.004>
- Grzelka, M.; Chajda, J.; Budzik, G.; Gessner, A.; Wieczorowski, M.; Staniek, R.; Gapiński, B.; Koterka, R.; Krasicki, P.; Marciniak, L. 2010. Optical coordinate scanners applied for the inspection of large scale housings produced in foundry technology, *Archives of Foundry Engineering* 49(1): 255–260.
- Grzelka, M.; Majchrowski, R.; Sadowski, Ł. 2011. Investigations of concrete surface roughness by means of 3D scanner, in *Proc. of Electrotechnical Institute* 58(251): 97–107.
- Hasanzadehshooili, H.; Lakirouhani, A.; Šapalas, A. 2012. Neural network prediction of buckling load of steel arch-shells, *Archives of Civil and Mechanical Engineering* 12(4): 477–484.  
<http://dx.doi.org/10.1016/j.acme.2012.07.005>
- Hoła, J.; Sadowski, Ł. 2012. Testing interlayer pull-off adhesion in concrete floors by means of non-destructive acoustic methods, in *The 18th World Conference on Nondestructive Testing*, 16–20 April, 2012, Durban, South Africa, 8 p.
- Hoła, J.; Sadowski, Ł.; Schabowicz, K. 2011. Nondestructive identification of delaminations in concrete floor toppings with acoustic methods, *Automation in Construction* 20(7): 799–807.  
<http://dx.doi.org/10.1016/j.autcon.2011.02.002>
- Hoła, J.; Schabowicz, K. 2005. Application of artificial neural networks to determine concrete compressive strength based on non-destructive tests, *Journal of Civil Engineering and Management* 11(1): 23–32.
- Hoła, J.; Schabowicz, K. 2010. State-of-the-art non-destructive methods for diagnostic testing of building structures – anticipated development trends, *Archives of Civil and Mechanical Engineering* 10(3): 5–18.
- Kaczmarczyk, L.; Waszczyszyn, Z. 2007. Identification of characteristic length of microstructure for second order continuum multiscale model by Bayesian neural networks, *Computer Assisted Mechanics and Engineering Sciences* 14(2): 183–196.
- Kaliszuk, J.; Urbańska, A.; Waszczyszyn, Z.; Furtak, K. 2001. Neural analysis of concrete fatigue durability on the basis of experimental evidence, *Archives of Civil Engineering* 47(3): 327–339.
- Kappatos, V. A.; Dermatas, E. S. 2007. Feature extraction for crack detection in rain conditions, *Journal of Nondestructive Evaluation* 26(2): 57–70.  
<http://dx.doi.org/10.1007/s10921-007-0020-2>
- Kim, K.-B.; Sim, K.-B.; Ahn, S.-H. 2006. Recognition of concrete surface cracks using the ART1-based RBF network, *Lecture Notes in Computer Science* 3972: 669–675.
- Kuzinovski, M.; Tomov, M.; Cichosz, P. 2009. Effect of sampling spacing upon change of hybrid parameters values of the roughness profile, *Journal of Production Engineering* 12(1): 23–27.
- Kwaśnicka, H. 2005. *Sztuczna inteligencja i systemy ekspercyjne. Rozwój, perspektywy* [Artificial intelligence and expert systems. Development and prospects]. Wrocław: College of Management and Finances. 188 p.
- Łowińska-Kluge, A.; Błaszczyszynski, T. 2012. The influence of internal corrosion on the durability of concrete, *Archives of Civil and Mechanical Engineering* 12(2): 219–227.
- Łukowski, P. 2005. Przyczepność betonopodobnych kompozytów polimerowo-cementowych do podłoża [Adhesion of polymer-cement concretes to the substrate], *Cement Wapno Beton* 3: 142–147.
- Mathia, T. G.; Pawlus, P.; Wieczorowski, M. 2011. Recent trends in surface metrology, *Wear* 271(3–4): 494–508.  
<http://dx.doi.org/10.1016/j.wear.2010.06.001>
- Matsuyama, K.; Yamada, M.; Ohtsu, M. 2010. On-site measurement of delamination and surface crack in concrete structure by visualized NDT, *Construction and Building Materials* 24(12): 2381–2387.  
<http://dx.doi.org/10.1016/j.conbuildmat.2010.05.011>
- Moody, J.; Darken, C. J. 1989. Fast learning in networks of locally tuned processing units, *Neural Computation* 1(2): 281–294.  
<http://dx.doi.org/10.1162/neco.1989.1.2.281>
- Naderi, M.; Ghodousian, O. 2012. Adhesion of self-compacting overlays applied to different concrete substrates and its prediction by fuzzy logic, *The Journal of Adhesion* 88(10): 848–865.  
<http://dx.doi.org/10.1080/00218464.2012.705673>
- Ottosen, N.; Ristinmaa, M.; Davis, A. 2004. Theoretical interpretation of impulse response tests of embedded

- concrete structures, *Journal of Engineering Mechanics* ASCE 130(9): 1062–1071.  
[http://dx.doi.org/10.1061/\(ASCE\)0733-9399\(2004\)130:9\(1062\)](http://dx.doi.org/10.1061/(ASCE)0733-9399(2004)130:9(1062))
- Ourahmoune, R.; Salvia, M.; Mathia, T.; Berthel, B.; Fouvry, S.; Mesrati, N. 2011. Effect of sandblasting substrate treatment on single lap shear strength of adhesively bonded PEEK and its composites, in *The 18th International Conference on Composite Materials*, 2011, Jeju, Korea, 6 p.
- Piotrowski, T. 2009. *Zastosowanie analizy sygnału impact-echo do oceny jakości zespolenia w układach naprawczych betonu* [The use of the impact-echo signal to assess bond quality in concrete repair systems]. PhD thesis. Warsaw: Warsaw University of Technology.
- Rafajłowicz, E.; Skubalska-Rafajłowicz, E. 2009. RBF nets for approximating an object's boundary by image random sampling, *Nonlinear Analysis, Theory, Methods & Applications* 71(12): e1247–e1254.  
<http://dx.doi.org/10.1016/j.na.2009.01.155>
- Reiner, J.; Stankiewicz, M. 2011. Evaluation of the predictive segmentation algorithm for the laser triangulation method, *Metrology and Measurement Systems* 18(4): 667–678.
- Sadowski, Ł. 2012. *Nieniszcząca ocena zespolenia warstw betonowych w podlogach z wykorzystaniem sztucznych sieci neuronowych* [Non-destructive evaluation of bond between concrete layers in floors by means of artificial neural networks]. PhD thesis. Wrocław: Wrocław University of Technology.
- Sadowski, Ł. 2013. Non-destructive investigation of corrosion current density in steel reinforced concrete by artificial neural networks, *Archives of Civil and Mechanical Engineering* 13(1): 104–111.  
<http://dx.doi.org/10.1016/j.acme.2012.10.007>
- Sasse, H. 2007. Polymer adhesion to concrete – theories and engineering aspects, in Czarniecki, L.; Garbacz, A. *Adhesion in Interfaces of Building Materials: a Multi-scale Approach*, Advances in Materials Science and Restoration, No. 2, Aedificatio Publishers, 7–19.
- Schabowicz, K. 2003. *Nieniszcząca identyfikacja wytrzymałości na ściskanie betonu z wykorzystaniem sztucznych sieci neuronowych* [Non-destructive identification of the compressive strength of concrete by means of artificial neural networks]. PhD thesis. Wrocław: Wrocław University of Technology.
- Shaw, M. R.; Millard, S. G.; Molyneaux, T. C. K.; Taylor, M. J.; Bungey, J. H. 2005. Location of steel reinforcement in concrete using ground penetrating radar and neural networks, *NDT & E International* 38(3): 203–212.  
<http://dx.doi.org/10.1016/j.ndteint.2004.06.011>
- Siewczyńska, M. 2012. Method for determining the parameters of surface roughness by usage of a 3D scanner, *Archives of Civil and Mechanical Engineering* 12(2): 83–89. <http://dx.doi.org/10.1016/j.acme.2012.03.007>
- Werner, S.; Neumann, I.; Thienel, K.-C.; Heunecke, O. 2013. A fractal-based approach for the determination of concrete surfaces using laser scanning techniques: a comparison of two different measuring systems, *Materials and Structures* 46(1–2): 245–254.  
<http://dx.doi.org/10.1617/s11527-012-9898-y>
- Xie, T.; Yu, H.; Hewlett, J.; Różycki, P.; Wilamowski, B. M. D. 2012. Fast and efficient second-order method for training radial basis function networks, *IEEE Transactions on Neural Networks and Learning Systems* 23(4): 609–619.  
<http://dx.doi.org/10.1109/TNNLS.2012.2185059>
- Yao, W.; Chen, X.-Q.; Zhao, Y.; van Tooren, M. 2012. Concurrent subspace width optimization method for RBF neural network modeling, *IEEE Transactions on Neural Networks and Learning Systems* 23(2): 247–259.  
<http://dx.doi.org/10.1109/TNNLS.2011.2178560>
- Zapata, J.; Vilar, R.; Ruiz, R. 2012. Automatic inspection system of welding radiographic images based on ANN under a regularisation process, *Journal of Nondestructive Evaluation* 30(1): 34–45.  
<http://dx.doi.org/10.1007/s10921-011-0118-4>
- Zhang, G.; Harichandran, S.; Ramuhalli, P. 2011. Application of noise cancelling and damage detection algorithms in NDE of concrete bridge decks using impact signals, *Journal of Nondestructive Evaluation* 30(4): 259–272. <http://dx.doi.org/10.1007/s10921-011-0114-8>

**Łukasz SADOWSKI.** (MSc, Eng), a researcher at Wrocław University of Technology, Poland. He obtained his diploma in civil engineering at WUT in 2007. He is a research assistant at WUT, Institute of Building Engineering. Research interests: concrete (especially concrete floors), non-destructive tests, acoustic techniques and artificial intelligence.